Report No. K-TRAN: KSU-20-3 ▪ FINAL REPORT ▪ May 2026

Initial Analytical Investigation of Cantilever and Butterfly Steel Overhead Sign Trusses with Respect to Remaining Fatigue Life

Khalid W. Al Shboul
Hayder A. Rasheed, Ph.D., P.E.

Kansas State University Transportation Center

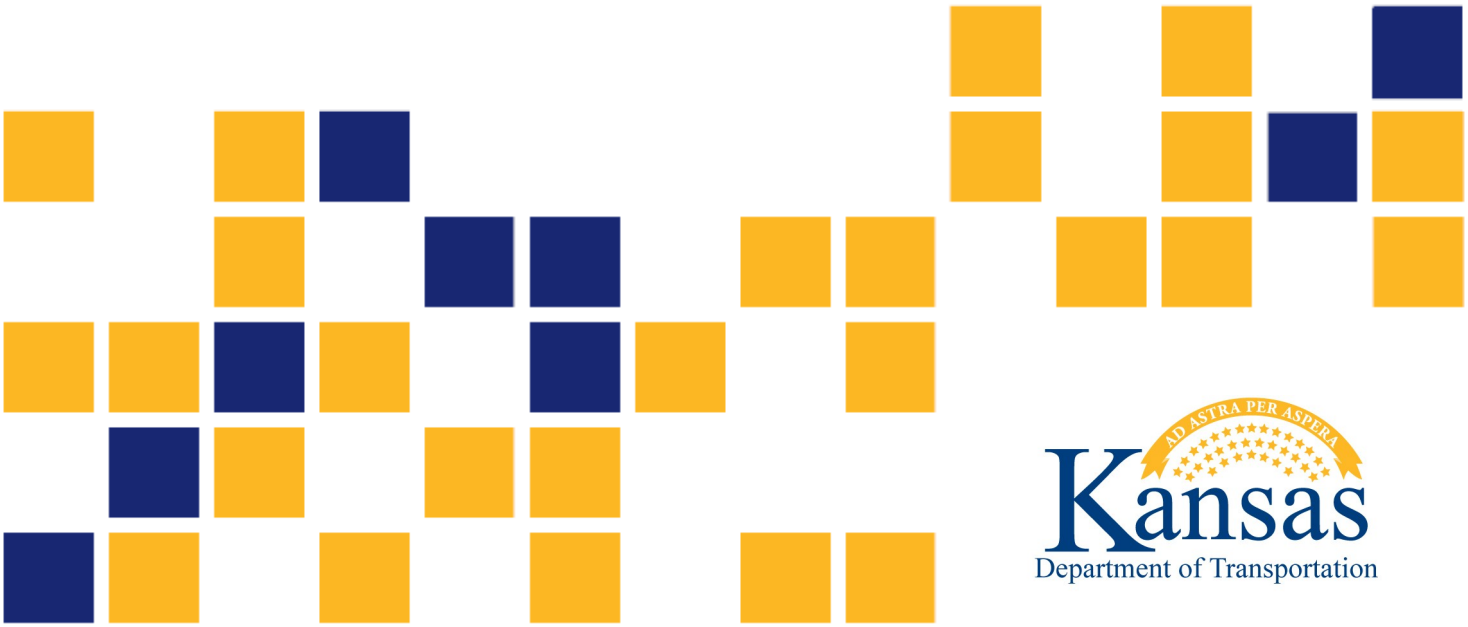

Kansas
Department of Transportation

1 Report No. K-TRAN: KSU-20-3	**2 Government Accession No.**	**3 Recipient Catalog No.**
4 Title and Subtitle Initial Analytical Investigation of Cantilever and Butterfly Steel Overhead Sign Trusses with Respect to Remaining Fatigue Life		**5 Report Date** May 2026 **6 Performing Organization Code**
7 Author(s) Khalid W. Al Shboul; Hayder A. Rasheed, Ph.D., P.E.		**8 Performing Organization Report No.**
9 Performing Organization Name and Address Kansas State University Transportation Center Civil Engineering Department Fiedler Hall Manhattan, KS 66506-5000		**10 Work Unit No. (TRAIS)** **11 Contract or Grant No.** C2144
12 Sponsoring Agency Name and Address Kansas Department of Transportation Bureau of Research 2300 SW Van Buren Topeka, Kansas 66611-1195		**13 Type of Report and Period Covered** Final Report August 2019 – May 2022 **14 Sponsoring Agency Code** RE-0789-01
15 Supplementary Notes For more information write to address in block 9.		

16 Abstract

Fatigue failure of highway sign structures due to sustained wind-loading events has been recognized in many states. In fact, the American Association of State Highway and Transportation Officials specifies that the structural component should be designed for infinite life by maintaining wind-induced stress below their constant amplitude fatigue threshold. However, because existing structures are typically not designed for fatigue, the condition of all critical and fatigue-prone components must be evaluated for safety. Visual inspection requires extensive time and effort and may not detect unnoticed fatigue cracks, so growing attention has focused on analytical inspection tools to examine all critical members and connections for remaining fatigue life to ensure public safety. The reliability of these analytical tools depends on the accuracy of wind-loading models applied during the life span of the structure. This study devised a fill-interpolate-extend approach to furnish a wind-loading data ensemble for the duration of analysis. The ensemble established a reliable synthetic wind model to generate fatigue cycle counts. In addition, a comprehensive analytical framework, including structural modeling, stress extraction/processing, and fatigue damage simulation, was integrated to yield an affordable tool that is applicable to various sign structures topologies. The resulting software for non-cantilever overhead structures as well as cantilever and butterfly assemblies were successfully verified to predict real cases for fatigue damage, reflecting the in-situ condition of the structures.

17 Key Words Overhead traffic signs, Sign supports, Structural supports, Trusses, Cantilevers		**18 Distribution Statement** No restrictions. This document is available to the public through the National Technical Information Service www.ntis.gov.	
19 Security Classification (of this report) Unclassified	**20 Security Classification (of this page)** Unclassified	**21 No. of pages** 55	**22 Price**

Form DOT F 1700.7 (8-72)

This page intentionally left blank.

Initial Analytical Investigation of Cantilever and Butterfly Steel Overhead Sign Trusses with Respect to Remaining Fatigue Life

Final Report

Prepared by

Khalid W. Al Shboul
Hayder A. Rasheed, Ph.D., P.E.

Kansas State University Transportation Center

A Report on Research Sponsored by

THE KANSAS DEPARTMENT OF TRANSPORTATION
TOPEKA, KANSAS

and

KANSAS STATE UNIVERSITY TRANSPORTATION CENTER
MANHATTAN, KANSAS

May 2026

PREFACE

The Kansas Department of Transportation's (KDOT) Kansas Transportation Research and New-Developments (K-TRAN) Research Program funded this research project. It is an ongoing, cooperative and comprehensive research program addressing transportation needs of the state of Kansas utilizing academic and research resources from KDOT, Kansas State University and the University of Kansas. Transportation professionals in KDOT and the universities jointly develop the projects included in the research program.

NOTICE

The authors and the state of Kansas do not endorse products or manufacturers. Trade and manufacturers names appear herein solely because they are considered essential to the object of this report.

This information is available in alternative accessible formats. To obtain an alternative format, contact the Office of Public Affairs, Kansas Department of Transportation, 700 SW Harrison, 2nd Floor – West Wing, Topeka, Kansas 66603-3745 or phone (785) 296-3585 (Voice) (TDD).

DISCLAIMER

The contents of this report reflect the views of the authors who are responsible for the facts and accuracy of the data presented herein. The contents do not necessarily reflect the views or the policies of the state of Kansas. This report does not constitute a standard, specification or regulation.

Abstract

Fatigue failure of highway sign structures due to sustained wind-loading events has been recognized in many states. In fact, the American Association of State Highway and Transportation Officials specifies that the structural component should be designed for infinite life by maintaining wind-induced stress below their constant amplitude fatigue threshold. However, because existing structures are typically not designed for fatigue, the condition of all critical and fatigue-prone components must be evaluated for safety. Visual inspection requires extensive time and effort and may not detect unnoticed fatigue cracks, so growing attention has focused on analytical inspection tools to examine all critical members and connections for remaining fatigue life to ensure public safety. The reliability of these analytical tools depends on the accuracy of wind-loading models applied during the life span of the structure. This study devised a fill-interpolate-extend approach to furnish a wind-loading data ensemble for the duration of analysis. The ensemble established a reliable synthetic wind model to generate fatigue cycle counts. In addition, a comprehensive analytical framework, including structural modeling, stress extraction/processing, and fatigue damage simulation, was integrated to yield an affordable tool that is applicable to various sign structures topologies. The resulting software for non-cantilever overhead structures as well as cantilever and butterfly assemblies were successfully verified to predict real cases for fatigue damage, reflecting the in-situ condition of the structures.

Acknowledgments

This research was made possible through funding from the Kansas Transportation Research and New-Developments (K-TRAN) Research Program from the Kansas Department of Transportation (KDOT). Thanks are extended to KDOT team members in the Bureau of Structural and Geotechnical Services who supported the project during all its development stages. Special thanks are extended to Karen Peterson, Eric Anderson, and Mark Hurt.

Table of Contents

List of Tables

List of Figures

Chapter 1: Introduction

1.1 Background

Full-span sign support structures are frequently used on major highways to guide road users. These structures typically extend over multiple lanes to provide necessary information to all road users and prevent hazards resulting from collisions. Because sign structures are flexible due to their long span length and relatively small cross sections and mass, they have very low natural frequencies and minimal damping, making them susceptible to significant amplitude vibration. Large-amplitude oscillation does not necessarily negatively impact the integrity of the design, but many motorists complain when the displacement range exceeds 8 in. (200 mm) because they cannot see the signals or signs and are concerned about driving under vibrating structures according to the American Welding Society (AWS D1.1-2000, 2000). The most significant concern, however, is that stress fluctuations in structure details can lead to fatigue cracking. Many state departments of transportation (DOTs) have reported cracks in sign structures and even sign structure failure due to fatigue damage (Dexter & Ricker, 2002). Figures 1.1 and 1.2 show examples of fatigue failure on different highway sign structures.

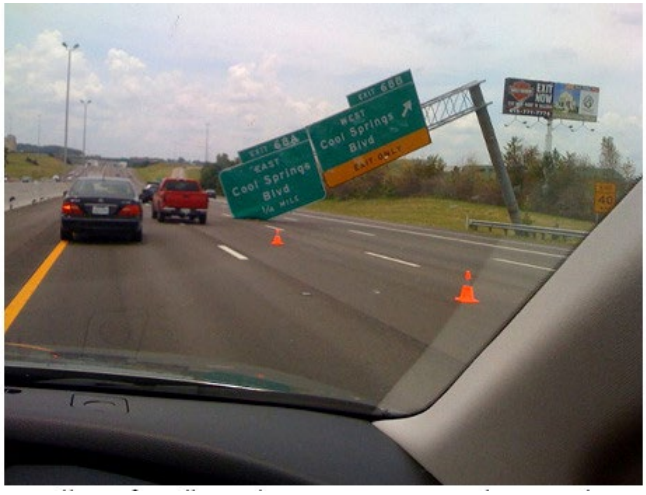

Figure 1.1: Failure of Cantilever Sign Support Structure in Tennessee
Source: Beneberu et al. (2014)

Figure 1.2: Fatigue Failure at Mast Arm Connection of Traffic Signal
Source: Florea et al. (2007)

The Kansas Department of Transportation (KDOT) typically uses cantilevered, double cantilevered, and overhead sign structure topologies throughout the roadway system. Although each structure type is equipped with fatigue-sensitive connections where fatigue damage tends to occur, most sign structures in Kansas have been in service for more than 45 years, meaning they were not originally designed to prevent fatigue. Therefore, routine fatigue inspections of all structural components must be conducted to ensure structural integrity and to repair or replace any defective elements. These inspections must be thorough and comprehensive to eliminate all fatigue cracks, which means the inspection plans are tedious and complex due to the many members that must be evaluated. Consequently, a more reliable methodology is needed to efficiently inspect and evaluate these structures to identify critical fatigue cracks. This study aimed to develop a comprehensive approach for fatigue inspection from wind-loading development to model, analyze, and structurally assess various components in highway sign structures.

1.2 Objectives

Low-cost cantilevered and butterfly sign support structures are commonly used because they more effectively reduce the probability of vehicle collision compared to overhead sign structures. Over time, the span of cantilevered support structures has increased as safety concerns have caused the upright component of the structures to be installed further from the road, see Figure 1.1–1.2. However, because these structures are typically used for multi-lane roads, the structures are increasingly susceptible to large amplitude oscillations from various wind-loading scenarios. Therefore, this study evaluated the remaining fatigue life of cantilevered and butterfly

structures to build a comprehensive tool to accurately predict the remaining fatigue life of cantilevered and butterfly highway sign support structures subjected to prolonged and sustained wind fluctuations. The analytical study sought to obtain the following specified objectives:

- Develop fatigue analysis procedures to estimate the fatigue life expectancy of cantilevered and butterfly sign structures and evaluate the remaining fatigue life of these structures based on the wind-loading dataset generated above.
- Identify and mark the most critical members in the various sign structures for further field investigation concerning fatigue life consumption.
- Project the number of years these structures would experience total fatigue damage and guide highway agencies to prioritize their inspection plans.
- Develop a computationally affordable simulation package using object-oriented programming language C# to interact with the FE software STAAD Pro to predict fatigue life.

1.3 Scope

This report consists of four chapters. The first chapter introduces the topic, objectives of the work, and the scope of the research. Chapter 2 includes a literature review, and Chapter 3 extends the developed methodology to other flexible structures, namely cantilevered and butterfly highway structures, and evaluates the applicability of this method for identifying fatigue damage in various connection members in correlation with the structural software. Conclusions and recommendations are presented in Chapter 4.

Chapter 2: Literature Review

A brief overview regarding the work conducted on the fatigue inspection of highway sign structures is introduced in this chapter.

2.1 Fatigue Damage of Highway Sign Structures

The repeated loading and unloading of members and connections in highway sign structures makes these structures susceptible to the accumulation of fatigue damage, which can ultimately lead to fatigue failure. Therefore, these structures must be designed to endure typical in-service loading scenarios while maintaining a level of accumulated fatigue damage below an acceptable limit. To ensure that support structures are proportioned to withstand all wind-induced loading scenarios and that wind-induced stresses are below the constant amplitude fatigue threshold (CAFT), AASHTO (2015) specifications require sign support structures to be designed for fatigue using two approaches: nominal stress-based classifications of typical connection details or experiment-based methodologies.

Previous studies have provided reasonably detailed methods of quantifying fatigue damage in highway sign structures, including fatigue simulations using various wind-loading scenarios, structure types, and analysis methods (Alshareef et al., 2022; Chen et al., 2001; Creamer et al., 1979; DeSantis & Haig, 1996; Dexter & Ricker, 2002; Fouad & Hosch, 2011; Hong et al., 2016; Letchford & Cruzado, 2008). For example, Creamer et al. (1979) studied the effects of truck-induced gusts on one double cantilever (butterfly) structure and two standard double-mast arm cantilever structures. The structure response and member forces due to the vehicle-induced gusts were experimentally investigated, and they analytically and numerically studied the static and dynamic behavior of the sign structures to determine an appropriate gust load to simulate measured field response. They suggested the use of category C CAFT to achieve infinite life for double-nutted anchor bolts.

In the National Cooperative Highway Research Program (NCHRP) Report 412, Kaczinski et al. (1998) characterized the susceptibility of cantilevered structures to excessive displacement, or fatigue damage, to develop equivalent static load ranges for four common wind-related causes of fatigue, identify fatigue-sensitive connection details in a sign structure, and determine the

fatigue strength of anchor bolts. Results revealed at least four wind-loading phenomena that can produce significant displacements and stress ranges in cantilever sign structures: galloping, vortex shedding, natural wind gusts, and truck-induced wind gusts. These four loading types were shown to significantly contribute to fatigue damage of sign structures. To determine susceptibility to galloping and vortex shedding, the authors performed wind-tunnel testing of scale models of five representative structures. Three of the structures were cantilevered mast arms (one supporting two traffic lights, one supporting one traffic light, and one with a sign), while the others were two chord trusses (both supporting a single sign). The structures were tested with and without sign attachments. Results showed that infrequent galloping-induced vibrations depend on the condition of the specific structure, but they produce persistent vibration. The authors recommended that a shear pressure range of 21 psf (1000 Pa) be applied vertically to the vertically projected area of any attachment to prevent galloping of cantilevered structures. Overhead structures were shown to be less susceptible to galloping. Study results also showed that vortex shedding should only be considered before the attachments (i.e., signs or lights) are fastened to the structure and that only structures with horizontal supports of large diameter are prone to such phenomena.

The second goal of the research by Kaczinski et al. (1998) was to categorize fatigue-sensitive connection details with respect to AASHTO fatigue design curves (AASHTO, 1994). Therefore, the researchers grouped details with similar cracking modes and similar stress concentrations into categories A–E', where the fatigue threshold of the detail decreased in alphabetical order. A majority of the details on a cantilevered sign were in categories E or E', although anchor bolts were in category D.

Repetto and Solari (2001) proposed a mathematical model to derive a histogram of stress cycles, accumulated damage, and the fatigue life of slender vertical structures in the along-wind vibration direction. The response of the vertical structures was treated as a narrow-band process, which simplified the representation of wind velocity. The method broke down the broad-band process of wind velocity and considered each small-time span as a narrow-band process of a mean wind speed plus variations. Natural wind was considered the load-causing fatigue damage.

Ginal (2003) investigated the fatigue performance of three full-span overhead sign support structures using ANSYS, considering natural wind load and truck-induced pressures. Results

showed that truck-induced pressures had minimal damaging effect on most full-span overhead sign structures, while natural wind-loading speeds of 20–50 mph had the most damaging effect. The predicted remaining life for the investigated structures was 4–27 years.

Kacin et al. (2010) performed fatigue analysis of pristine and damaged overhead four-chord truss sign structures using stress histories obtained from an FE solution to identify critical structural members. They used the Kaimal wind spectrum for base wind speeds of 5–25 mph. Infinite fatigue life was predicted for welded diagonal members, but they recommended field monitoring of the real structure and accurate field measuring of wind loading to confirm exact conditions of the structures.

2.2 Analytical Modeling of Natural Wind

The literature has investigated several techniques to model the power spectral density function for turbulent wind speed for practical engineering applications. The classical model of the wind turbulence spectrum is attributed to Davenport (1961), in which he used approximately 70 spectra results of horizontal components of gust in intense wind events in various locations and circumstances worldwide. The Davenport model is given by:

$$S_D(f) = \frac{4U_*^2 x^2}{f(1+x^2)^{4/3}}$$

$$x = \frac{4000f}{U_z}$$

$$V(z) = V_{10}.(\frac{Z}{10})^{\alpha}$$

Equation 2.1

Where $S_D(f)$ is the fluctuation wind-speed spectrum, f is the frequency, z is the height, $V(z)$ is the mean wind speed at the height of z, V_{10} is the mean wind speed at the standard height of 10 m, α is the ground roughness exponent, k is the terrain roughness factor, and U_* is the friction (or shear) velocity.

The friction velocity accounts for wind speed turbulence resulting from interference with the ground surface. According to Equation 2.1, the Davenport model is independent of height above the ground surface, so wind turbulence generated with this spectrum is fixed to a mean velocity at a particular reference height. However, this reference height may not coincide with the height of the structure under consideration, so subsequent researchers have suggested improved models that are height dependent.

Various researchers have modified the Davenport model to account for the structure height above the ground surface and the accuracy of structural response within different frequency ranges. For example, the spectral density of the turbulent wind component proposed by Kaimal et al. (1972) accounts for the height of the structure:

$$S_K(f) = \frac{200U_*^2 z}{U_z\left(1 + 50\frac{fz}{U_z}\right)^{5/3}}$$

Equation 2.2

Where S_K is the Kaimal spectrum, z is the height above the ground (10 m = 33 ft), U_* is shear velocity, U_z is the mean wind velocity at z, and f is the specified frequency.

The wind turbulence spectrum given by Equation 2.2 is superior to the Davenport spectrum and is an acceptable model for most structural engineering applications. The Kaimal spectrum, which includes the effect of height on the turbulent wind component, has been found to be accurate in the high frequency response range of most engineered structures (Simiu & Scanlan, 1996).

Kumar and Stathopoulos (1997) presented a general approach for representing Gaussian and non-Gaussian wind pressure characteristics using the fast Fourier transform algorithm. The simulation procedure required Fourier amplitudes and phases to generate pressure time histories. The amplitudes were constructed from pressure spectra, and the phases were obtained from a stochastic model. Ginal (2003) also modeled a time history of randomly varying wind speeds to apply to the FE models of three overhead sign structures. A wide range of mean wind speeds (5–50 mph) were used in the analysis, and a fluctuating component of wind was modeled using the Kaimal wind spectrum because, unlike the Davenport spectrum used in the study by Dexter and Ricker (2002), the Kaimal spectrum accounts for elevation. An equation based on the superposition

of cosine waves was then used to combine the mean and fluctuating component of wind into a wind-speed time history.

Similarly, Li et al. (2005) developed a wind-load time history for FE analysis of sign structures in Indiana. The range of wind speeds used in the analysis varied from 0 to 30 mph. A fast Fourier transform-based method was employed to create the time history, which required choosing a number of frequencies within the range of natural frequencies of structural mode shapes. The Kaimal spectrum was then used to determine the fluctuating component of the wind.

2.3 Spatial Variation and Interpolation of Wind Speeds

Weather data are generally recorded at specific locations, but spatial interpolation can be used to estimate wind speed values at other locations where the data is missing or incomplete. Various deterministic and geostatistical interpolation methods can approximate values for spatially continuous phenomena from measured values at limited sample points. Most spatial interpolation techniques are based on the concept that derived values are represented as the weighted average of measured values at the sample points. The general interpolation formula is:

$$\dot{Z}\,(x_\circ, y_\circ) = \sum_{i=1}^{n} w_i\, Z(x_i, y_i),$$

Equation 2.3

Where $\dot{Z}\,(x_\circ, y_\circ)$ represents the predicated value at a specific location $(x_\circ, y_\circ)$; $Z(x_i, y_i)$ represents the measured value at the sample point (x_i, y_i); w_i is the weight assigned to the sample point; and *n* is the number of sampling points used (Luo et al., 2008; Webster & Oliver, 2007).

Chapter 3: Fatigue Evaluation

Cantilever and butterfly sign support structures support large signs that are used to promote highway accessibility, efficiency, and traffic-flow safety. However, unexpected fatigue damage within a structure's connection details can lead to catastrophic failure, causing injuries, property damage, and road closures (Hosseini, 2013). Therefore, safety issues related to these sign support structures have prompted research and intensive field inspection, leading most DOTs to utilize ring-stiffened box connections in new projects due to their superior fatigue-loading resistance. This change is based on experimental NCHRP studies (Hamilton et al., 2004; Puckett et al., 2010; Roy et al., 2011). Despite study results, however, fillet-welded mast-to-arm connection details remain a popular alternative due to their cost-effectiveness and minimal fabrication effort. Unfortunately, these connections are classified as the most fatigue-prone details, meaning stress fluctuations due to natural wind loading may cause fatigue cracks at these locations.

Because computing comprehensive wind-induced stresses during lifetime loading events is impractical, AASHTO recommends an infinite life fatigue design approach to overcome design unreliability for highway structures. Each component should resist the equivalent static wind load to maintain a stress level below the CAFT. AASHTO (2015) implemented findings from the NCHRP project (Roy et al., 2011) to identify the CAFT required for infinite life design in which each connection detail is associated with a certain CAFT in a tabulated format.

Extensive research has evaluated the responses of highway sign structures and explained fatigue failure in terms of critical spots, crack growth, and mitigation (Creamer et al., 1979; DeSantis & Haig, 1996; Dexter & Ricker, 2002; Kaczinski et al., 1998). Barle et al. (2011) developed an FE failure analysis of a cantilever sign structure by modeling the extreme monotonic wind load and stress spectra of variable service loads to reveal estimated fatigue life and design improvements. Roda et al. (2015) conducted a comparison study of AASHTO 2015 standards and AASHTO 2001 standards using two design examples of overhead and cantilever highway structures. Results showed that AASHTO 2015 guidelines, which use reliability methods and statistical data to introduce resistance factors for applied loads, is a more rational design approach because fatigue loads are based on available data, rational probability, and risk models. Rice et al.

(2012) utilized a full-scale experimental approach to capture the structural response of four representative sign trusses and conducted an analytical study to assess truss response at full-design wind loads. Li (2005) carried out FE analysis using ANSYS to model and analyze various highway sign structures, including single mast arm and double-mast arm cantilever structures. Results showed that, although the double-mast arm cantilever sign structure is the most critical of the non-cantilevered structures, all the structures had infinite life. Tsai and Alipour (2021) monitored the long-term health of a traffic signal structure to characterize wind-induced behavior and fatigue-damage parameters; the monitored structure was unable to dampen the in-plane vibration, which resulted in fatigue-stress accumulation. Choi and Najm (2018) conducted a reliability-based fatigue assessment for potential crack initiation in cantilevered sign structure connection details using probability curves to determine inspection frequencies and maintenance strategies.

Most DOTs, including KDOT, inspect highway sign structures via site visits and produce an inventory for each structure. However, because these costly, time-consuming inspections are often not performed regularly and can pose potential hazards for the inspector, the potential for unnoticed fatigue damage and assembly failure increases. The Federal Highway Administration (FHWA) does not regulate sign inspections; instead, the agency allows each state to establish regulation standards. Consequently, DOTs have developed unique procedures for inventory management and inspection parameters.

Although fatigue characteristics of highway sign structures have been widely investigated and critical spots have been identified, fatigue behavior is highly variable and encompasses many uncertainties resulting from service load, environmental conditions, material properties, and pre-existing imperfections (Zheng & Ellingwood, 1998). Accurate lifetime wind-loading event approximation is a critical factor for minimizing the unreliability of fatigue life calculations, but characterization of these wind-load events over a lifetime is impractical due to the lack of stress fluctuation spectrum. Therefore, this study used previously developed analytical natural wind-time histories in Kansas and AASHTO fatigue life calculation procedures to produce an inspection tool to calculate fatigue life consumption in critical spots in cantilevered and double cantilevered (butterfly) structures. This report summarizes the analytical inspection procedures, emphasizing

analytical modeling, structural assessment, and software development. Additional details on wind-load event development may be found in Al Shboul et al. (2023).

3.1 Sign Structures Modeling

3.1.1 KDOT Highway Structures

KDOT utilizes cantilever and balanced doubled cantilever (butterfly) sign trusses of various sizes, as shown in Figure 3.1. These structures are characterized by a uniform or tapered hollow circular single post. The post mounts a two-chord steel truss comprised of multiple angle sections measuring 3 in. by 3 in. by 0.375 in., which are connected to the main chords by welded angle-to-gusset connections. Structure geometry varies based on the design models. Eight standard models are depicted in KDOT standards and classified as retired or new designs. The key detail that changed between both model designs is the mast-to-arm connection. In the retired designs, this connection consisted of a horizontal gusseted box connection fillet welded to the post and connected to the main chords via a bolted plate, as shown in Figure 3.2(a). The new designs, however, consist of ring-stiffened connections that encircle the post entirely, as shown in Figure 3.2(b). In addition to the mast arm connection, the design models have unique detail dimensions, including wall thickness, pipe diameter, and plate size. Table 3.1 summarizes the geometric properties for the eight design models.

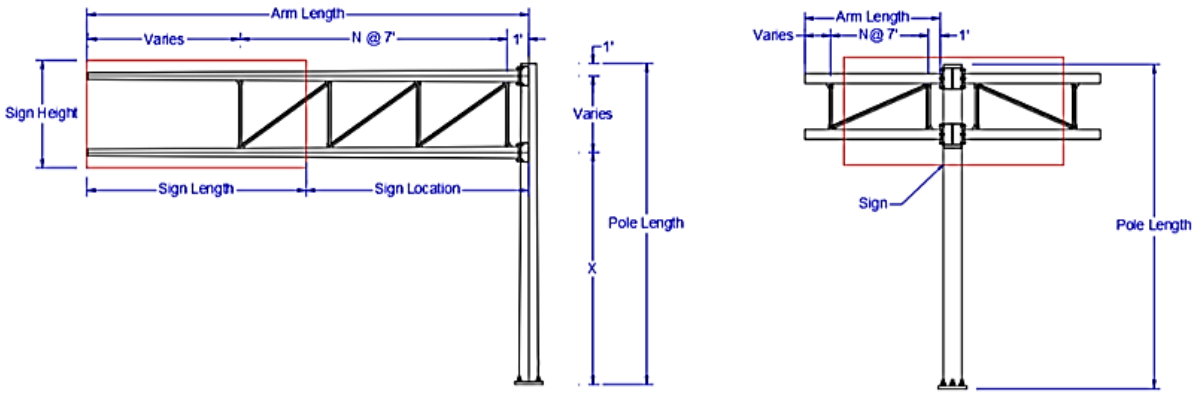

Figure 3.1: (a) Cantilever Model, (b) Butterfly Model

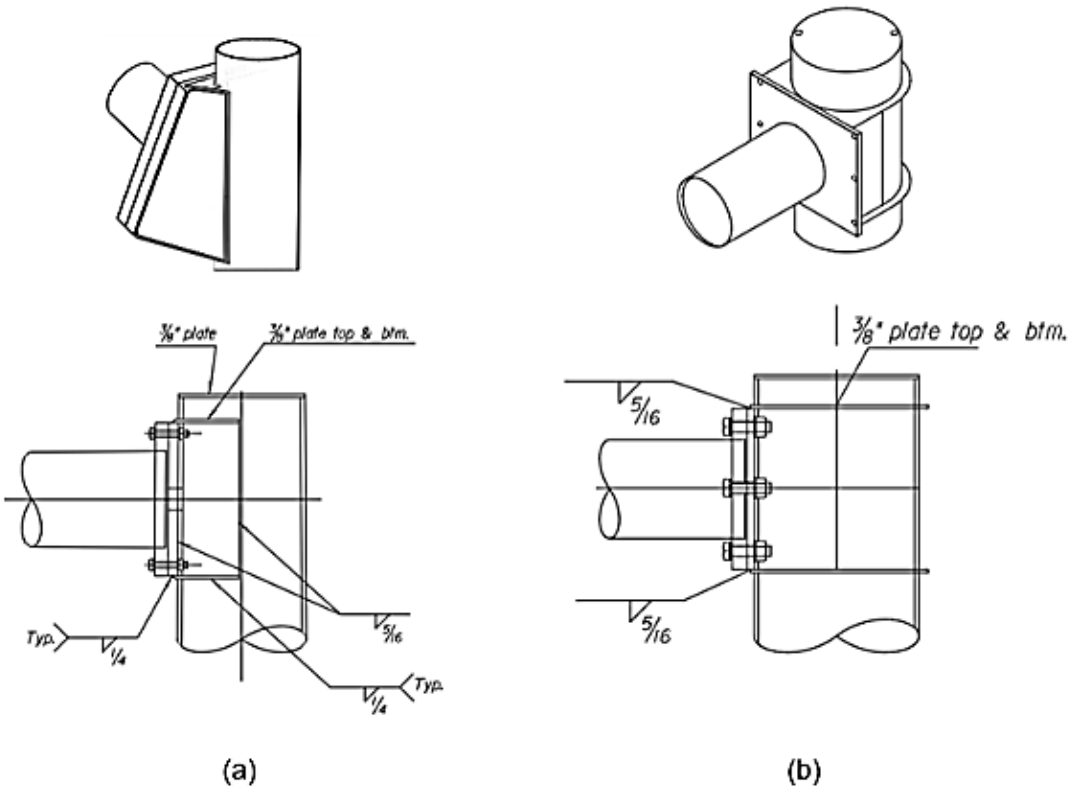

Figure 3.2: (a) Gusseted Box Connection, (b) Ring-Stiffened Box Connection

Table 3.1: Geometric Properties for Cantilever Models

Model	Post dimension	Arm dimension	A	Post uniformity	Arm to column connection
1	15" O.D × 3 Ga. wall	9.2" O.D × 3 Ga. wall	4'	Tapered / Uniform	Gusseted box connections
2	18" O.D × 3 Ga. wall	11.0" O.D × 7 Ga. wall	6'	Tapered / Uniform	Gusseted box connections
3	18" O.D × 3 Ga. wall	12.5" O.D × 7 Ga. wall	6'	Tapered / Uniform	Gusseted box connections
4	18" O.D × 3 Ga. wall	12.5" O.D × 7 Ga. wall	6'	Tapered / Uniform	Gusseted box connections
5	18" O.D × 3 Ga. wall	12.5" O.D × 3 Ga. wall	6'	Tapered / Uniform	Gusseted box connections
6	18" O.D × 3 Ga. wall	13.0" O.D × 3 Ga. wall	6'	Tapered / Uniform	Gusseted box connections
7	18" O.D × 3 Ga. wall	14.0" O.D × 5/8"	6'	Uniform	Ring-stiffened connections
8	20" O.D × 3 Ga. wall	14.0" O.D × 3/4"	6'	Uniform	Ring-stiffened connections

3.1.2 Finite Element Modeling

This study utilized the FE software Staad Pro V8i SS6 (Bentley Systems, 2016) to model flexible sign structures and execute a static analysis. The structures were modeled using a combination of beam elements, truss elements, and plate elements with actual or calibrated cross-sectional dimensions. The upper and lower main chords, which were modeled using a two-node frame element, ran continuously. The secondary members were simultaneously connected at the intersection nodes and released to act as a pin connection for rotations about the local y-axis, and the main truss chords were connected to plates that contained old and new connections. The base support was simulated as a fixed steel support with an elastic modulus of 29000 ksi.

The gusseted box connection was used in models 1–6 according to KDOT standards, while the ring-stiffened connection was used for models 7 and 8. A four-node plate element was used to model all the plates in the connection and attached directly to the main upper and lower chords at the center node. The steel plates, which had the same thicknesses as the actual structures, were connected to the post through another plate with the same fillet weld thickness and properties. The post was divided into sub-elements, and the plate nodes merged with post nodes, as shown in Figure 3.3. To verify that the connections were modeled correctly, the critical node deflections were calculated for nodes 18, 19, 24, 25, 26, and 27 for a specific model and compared to the results of the same model when the truss-post connection is taken as fully rigid. Beam elements were used to connect the post with the cantilevered truss, and the length of each beam was the post's radius at the connection level (for tapered post). The beam properties were Area = 1×10^6 in^2 and $I_x = I_y = I_z = 1\times10^8$ in^4. Geometry data are shown in Table 3.2.

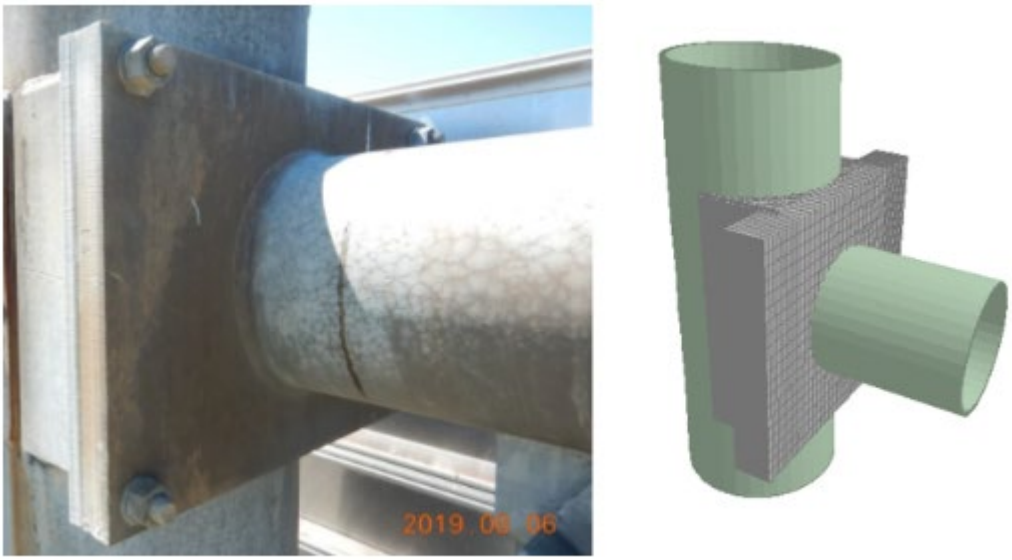

(a) (b)

Figure 3.3: (a) Post-to-Chord Connection, (b) FE Model of the Connection

Table 3.2: Geometry and Loading Data for the Test Model

Truss information		Sign information	
N	3	Location	2 ft
S	7 ft	Length	10 ft
Post height	10 ft	Height	8 ft
Wind speed	45 mph		

First-order structural analysis was performed on the rigid structure, gusseted box connection model, and ring-stiffened model, and the resulting responses were compared. Figure 3.4 shows the deflected shapes for the three models.

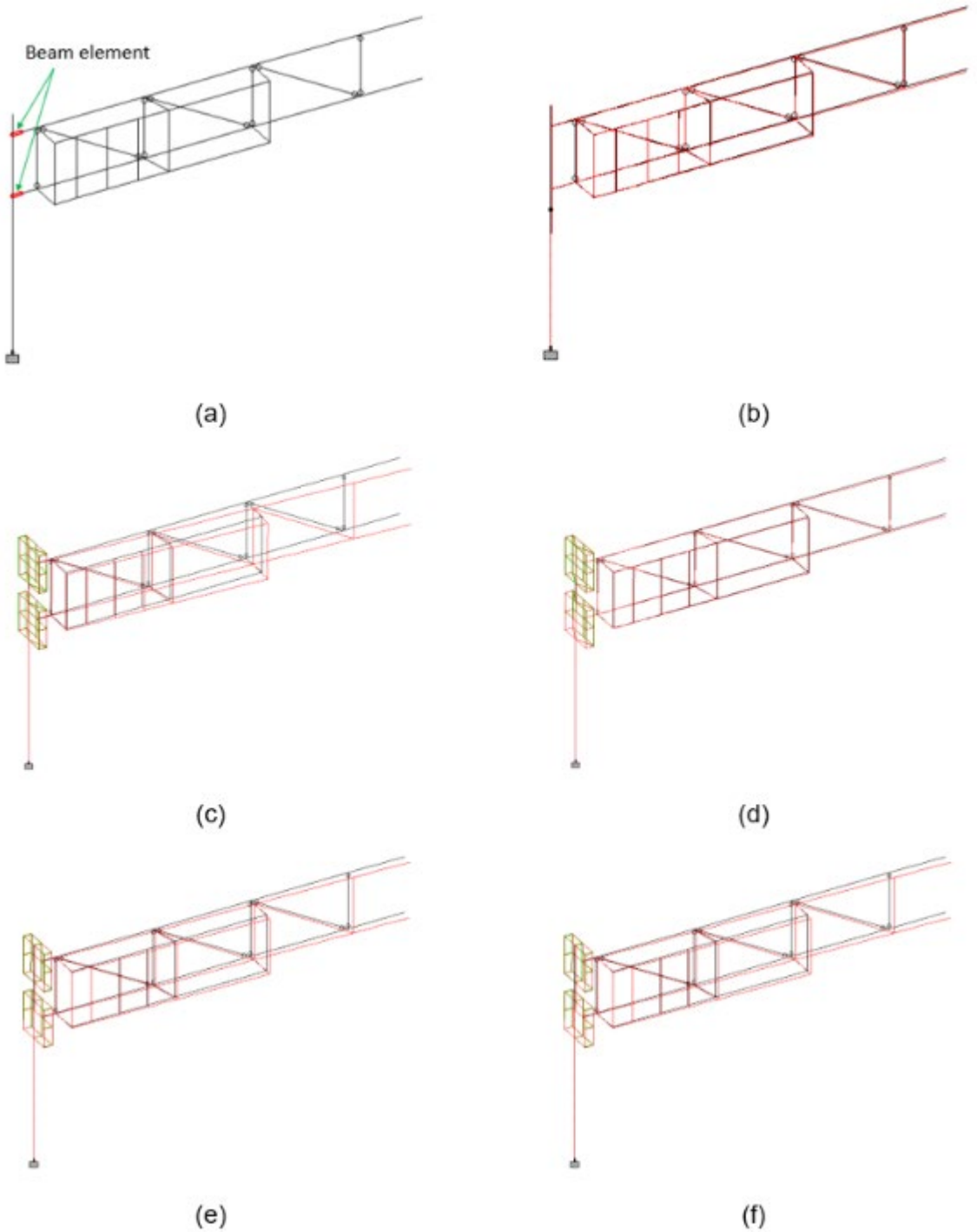

Figure 3.4: (a) Rigid Model, (b) Rigid-Dead Load, (c) Gusseted-Dead Load, (e) Ring-Stiffened-Normal Wind, (f) Gusseted-Dead Load

The analysis considered two load cases, dead load and normal wind load, on members, and joint displacements were recorded for six nodes near the post and at the tip of the cantilever.

Results are shown in Table 3.3 and Figure 3.5. Analysis results showed that the ring-stiffened connection and the gusseted box connection had almost the same response as the rigid theoretical connection in the Y direction due to the dead load. However, differences in the Z-direction deflection were observed due to the flexible nature of these connections. Overall, the connection modeling was reasonable.

Table 3.3: Key Nodes Deflection for Three Models

Model	Node	Load Case	X(mm)	Y(mm)	Z(mm)
Rigid connection	18	DEAD_LOAD_MEMBERS	7.186	-2.471	0.404
		NORMAL_WIND_MEMBERS	-0.000	0.003	17.307
	19	DEAD_LOAD_MEMBERS	13.724	-2.583	0.777
		NORMAL_WIND_MEMBERS	0.001	0.008	25.830
	24	DEAD_LOAD_MEMBERS	7.101	-37.859	0.271
		NORMAL_WIND_MEMBERS	0.102	0.298	137.162
	25	DEAD_LOAD_MEMBERS	13.762	-37.863	0.783
		NORMAL_WIND_MEMBERS	0.077	0.298	145.601
	26	DEAD_LOAD_MEMBERS	7.101	-44.604	0.243
		NORMAL_WIND_MEMBERS	0.102	0.319	161.640
	27	DEAD_LOAD_MEMBERS	13.762	-44.596	0.769
		NORMAL_WIND_MEMBERS	0.077	0.320	169.972
Gusseted box connection	18	DEAD_LOAD_MEMBERS	7.143	-2.612	0.380
		NORMAL_WIND_MEMBERS	-0.003	0.008	36.082
	19	DEAD_LOAD_MEMBERS	13.968	-2.686	0.801
		NORMAL_WIND_MEMBERS	-0.014	0.008	44.838
	24	DEAD_LOAD_MEMBERS	7.059	-39.462	0.285
		NORMAL_WIND_MEMBERS	0.089	0.258	382.543
	25	DEAD_LOAD_MEMBERS	14.005	-39.466	1.017
		NORMAL_WIND_MEMBERS	0.258	391.453	391.453
	26	DEAD_LOAD_MEMBERS	7.059	-46.490	0.278
		NORMAL_WIND_MEMBERS	0.089	0.274	450.178
	27	DEAD_LOAD_MEMBERS	7.143	-2.612	0.380
		DEAD_LOAD_MEMBERS	-0.003	0.008	36.082
Ring-stiffened connection	18	DEAD_LOAD_MEMBERS	7.143	-2.612	0.380
		NORMAL_WIND_MEMBERS	-0.003	0.008	36.082
	19	DEAD_LOAD_MEMBERS	13.968	-2.686	0.801
		NORMAL_WIND_MEMBERS	-0.014	0.008	44.838
	24	DEAD_LOAD_MEMBERS	7.059	-39.462	0.285
		NORMAL_WIND_MEMBERS	0.089	0.258	382.543
	25	DEAD_LOAD_MEMBERS	14.005	-39.466	1.017
		NORMAL_WIND_MEMBERS	0.258	391.453	391.453
	26	DEAD_LOAD_MEMBERS	7.059	-46.490	0.278
		NORMAL_WIND_MEMBERS	0.089	0.274	450.178
	27	DEAD_LOAD_MEMBERS	7.143	-2.612	0.380
		DEAD_LOAD_MEMBERS	-0.003	0.008	36.082

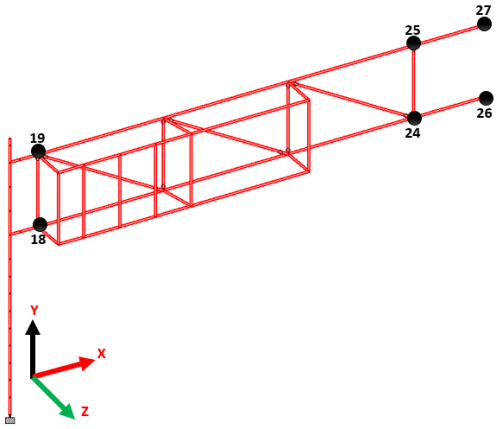

Key Nodes Label

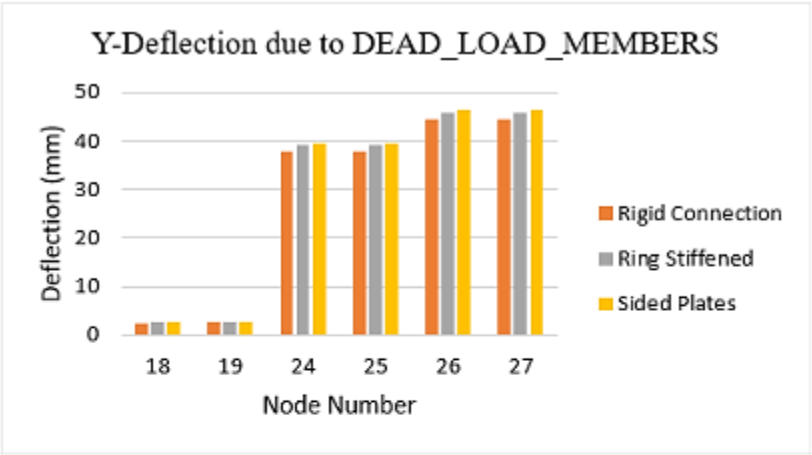

(a)

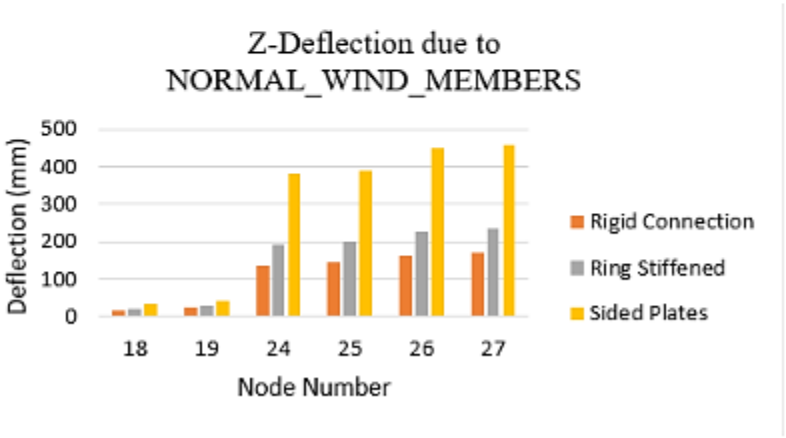

(b)

Figure 3.5: Key Nodes Deflection (a) Dead Load Case, (b) Normal Wind Load Case

A convergence study was then conducted to verify that the model converged and to determine the mesh size that provides a mesh-independent solution for the critical stress by comparing stresses obtained via different mesh densities. Figure 3.6 compares the stress for various mesh densities and mesh sizes. As shown in the figure, the mesh size with three elements across the height provided a stable converged solution. Because the developed approach can generate models with varying parameters and STAAD Pro can analyze multiple wind speeds, the three-element model was reproduced to yield the same results with less computational time. The three-element plate model was replaced by two plates along the connection height, and beam elements were connected to the two-sided plates at three locations (top, middle, and bottom). Figure 3.7 shows the beam locations and beam connections. Beam properties in the new support model were calibrated against the three-meshed support to yield the same stress at various spots and ensure that the structure's global response was identically the same.

Figure 3.8 compares the stress values for various locations in both models under different loading to ensure that the beam model yielded a consistent response. As shown, the stress in both models was identical, and the beam model connection provided satisfactory results. The trade-off between accuracy of results and computational time was acceptable and sufficient since many simulations will be carried out during the structure's service life span.

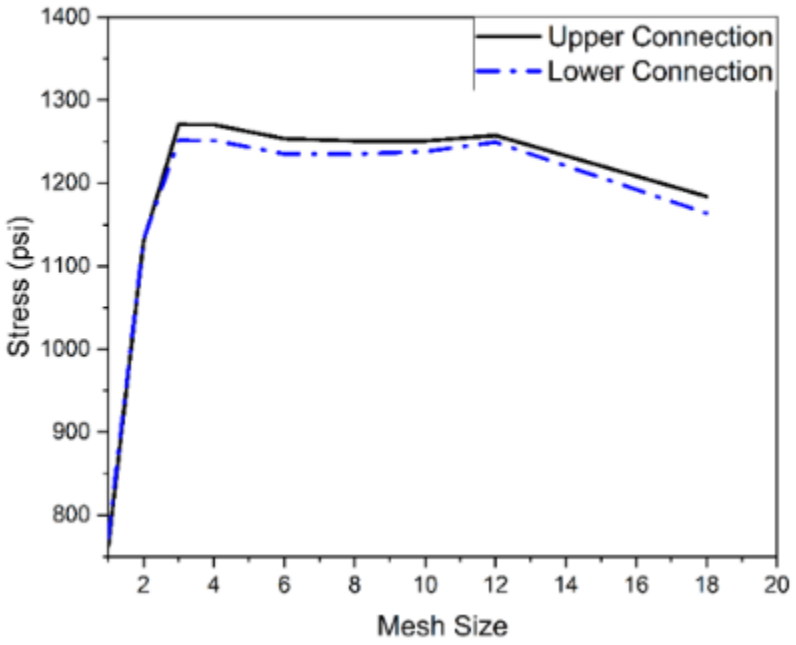

Figure 3.6: Stress at Plate Center Versus Mesh Density

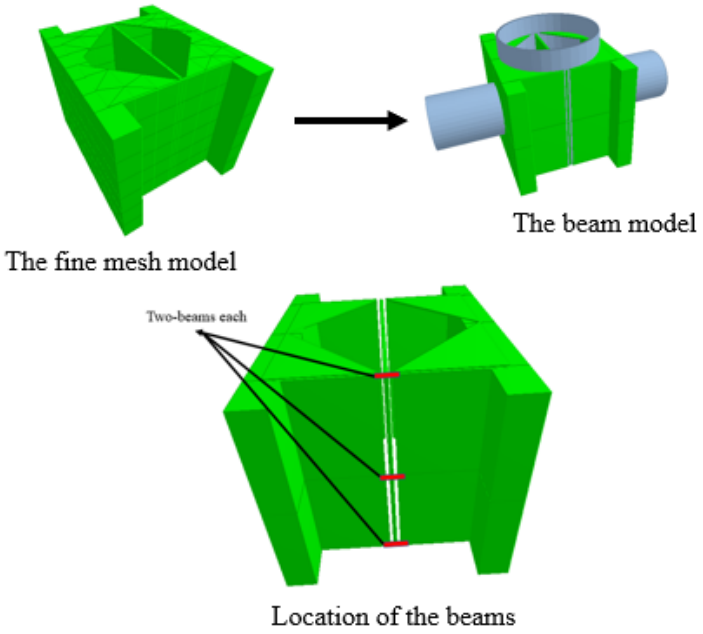

Figure 3.7: Calibrated Beam Connection

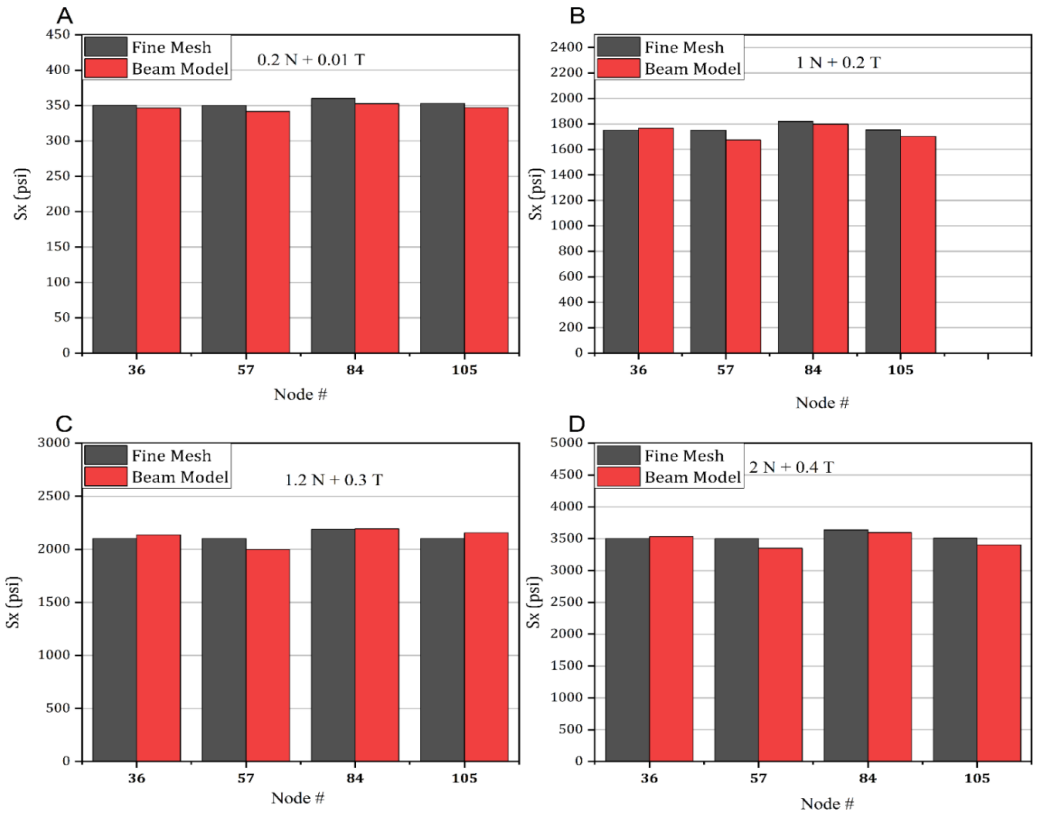

Figure 3.8: Stress Comparison in Various Locations for Beam Model Versus Fine-Meshed Model

If they are present on the truss, cantilever and butterfly assemblies typically support the sign(s), and sign placement varies with location, length, sign height, and the number of signs. Therefore, this study modeled the signs by creating a frame attached to the truss using four elements, with sign ribs distributed within the frame depending on the number and spacing of the ribs. The wind load was calculated based on the size of the sign and then distributed equally over the ribs. Since sign location is sensitive in the cantilever structure, the frame and ribs were created on the cantilever truss at their respective locations in the actual structure. The software can create intermediate nodes if needed to connect the sign frame to the primary chords of the truss.

3.2 Dynamic Amplification Factor (DAF)

This study utilized the static solution for an analytical model. Due to the dynamic nature of the wind, the calculated stresses were amplified using an overall blanket average (DAF). Analytical wind modeling was carried out over a range of frequencies (3–300 Hz), and, assuming

harmonic excitations, the DAF was calculated by averaging the frequency-response curve (Figure 3.9) for this range of frequencies, as in Equation 3.1:

$$DAF = \frac{\int_0^{1.4} \frac{dR}{\sqrt{(1-R^2)^2 + (2\xi R)^2}}}{1.4}$$

Equation 3.1

Where ξ is the damping ratio and R is

$\frac{\omega}{\omega_n}$ ω: *the excitation frequency*, ω_n: *natural frequency of the strucutre*.

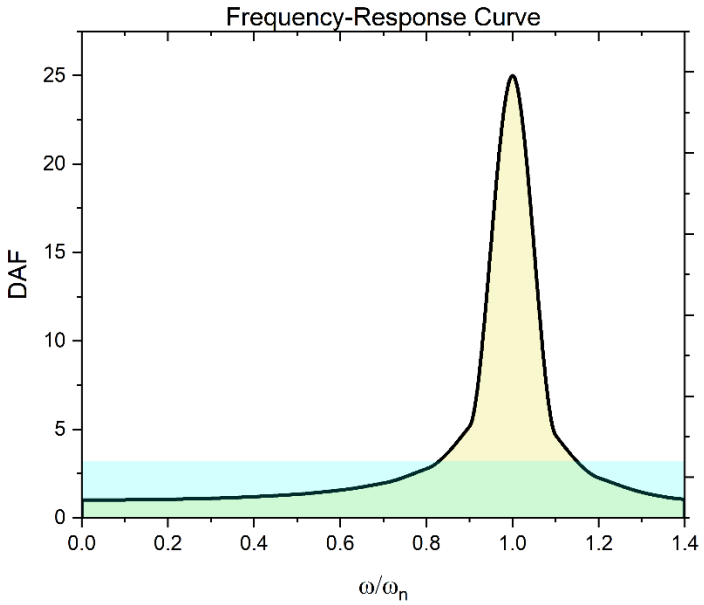

Figure 3.9: Frequency Response Curve and Average DAF ($\xi = 0.02$)

3.3 Wind Loading on Sign Structures

3.3.1 Synthetic Wind-Time Histories

Wind-speed records for Kansas were previously developed using isoparametric FE shape functions for all unsampled Kansas counties from available data recorded at 17 locations using the general interpolation formula in Equation 3.2 (Al Shboul et al., 2023):

$$\acute{Z}\,(x_\circ, y_\circ) = \sum_{i=1}^{n} w_i\, Z(x_i, y_i)$$

Equation 3.2

Where $\acute{Z}\,(x_\circ, y_\circ)$ represents the predicated value at a specific location $(x_\circ, y_\circ)$; $Z(x_i, y_i)$ represents the measured value at the sample point (x_i, y_i); w_i is the weight assigned to the sample point; and *n* is the number of sampling points used in the interpolation (Ben-Israel & Greville, 2003; Ye, 2013).

The developed wind-speed records were used to generate analytical wind-time histories to represent natural wind events during a structure's service life. The detailed interpolation method is described in Al Shboul et al. (2023). However, for convenience, the analytical derivation of the wind-time histories will be summarized here. A computational method using the Kaimal spectrum (Kaimal et al., 1972) was utilized to develop wind-time histories and generate each daily spectrum using Equation 3.3:

$$S_K(f) = \frac{200 U_*^2 z}{U_z \left(1 + 50 \frac{fz}{U_z}\right)^{5/3}}$$

Equation 3.3

Where S_K is the Kaimal spectrum, *z* is the height above the ground (33 ft (10 m)), U_* is the shear velocity, U_z is the mean wind velocity at *z*, and *f* is the specified frequency.

Fluctuation in the wind-time history was obtained by superimposing cosine waves over the entire frequency range and randomly generating phase angles using Equation 3.4 (Bobillier et al., 2001; Iannuzzi & Spinelli, 1987):

$$u(t) = \sum_{i=1}^{N} \sqrt{2 S_i f_i \Delta f}\,.\cos\,(2\pi f_i t + \emptyset_i)$$

Equation 3.4

Where $\emptyset_i$ is a randomly generated phase angle between 0 and 2π.

After generating the turbulence time history, the fluctuating function was combined with the mean wind speed on any given day to produce a complete wind-time history. The full-time history is given by:

$$U(t) = U_z + \sum_{i=1}^{N} \sqrt{2 S_i f_i \Delta f}\,.\cos\,(2\pi f_i t + \emptyset_i)$$

Equation 3.5

3.3.2 Wind-Loading Calculation

Wind loading resulting from certain wind speeds was evaluated by calculating the wind pressure using the following equation (AASHTO, 2015):

$$Pz = 0.00256K_z GV^2 I_r C_d \ (psf)$$

Equation 3.6

Where K_z is the height and exposure factor based on the height of the member and conservatively not less than 1.0. For example, if the structure is on a bridge, this value was 1.3. G is the gust factor = 1.14, V is the applied wind velocity (mph), and I_r is the importance factor = 1.0.

Drag coefficient (C_d) was based on the object size and shape. For truss members, the value of C_d was 1.2, while for the signs, the value of C_d was based on the aspect ratio. After generating the pressure resulting from each wind speed, the pressure was multiplied by the applicable area to generate wind force. The effect of the natural wind during the structure's service life was automated using the developed software, which can generate wind load and populate it to the Staad Pro models. Both effects of wind loading on signs and members were considered using AASHTO fatigue load cases.

3.4 Fatigue Damage Evaluation

3.4.1 AASHTO S-N Curves

This study utilized the *S-N* method to evaluate the fatigue life of various structural components using *S-N* curves for different connection types based on a wide range of laboratory fatigue tests of full-scale structures (AASHTO, 2015). Equation 3.7 expresses the number of cycles to failure:

$$N_i = \frac{A'}{\Delta\sigma_i^3}$$

Equation 3.7

Where N_i is the number of cycles to failure at *i–th* stress range, $\Delta\sigma_i$ is the member stress value corresponding to a wind speed value, and A' is a constant associated with the component provided in AASHTO (2015).

Table 3.4 describes *S*-*N* equations for components used in this study. In the table, each *S*-*N* curve has a flat plateau, or threshold, the stress is assumed to not contribute to the cumulative damage, and the components have infinite life.

Table 3.4: S-N Equations (AASHTO) for Structure Components

Description	A×10^8 (ksi^3)	Threshold (ksi)	Example	Location	Description	A×10^8 (ksi^3)	Threshold (ksi)	Example	Location
Plain material	250	24	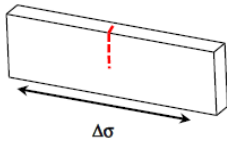	Post Members and truss main mem.	Fillet-welded tube-to transverse-plate connections	3.9	2.6	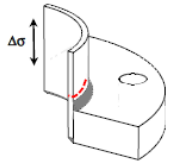	Base plate
Gusseted box connections	Infinite life	--	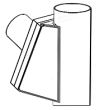	Mast Arm connection	Anchor bolts	22	7	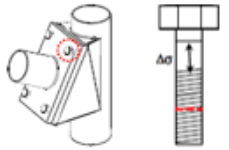	Connection bolts
Ring-Stiffened box connections	Infinite life	--		Mast arm connection	Partial-penetration groove-welded mast-arm-to-column pass-through connections	11	4.5	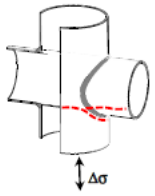	Arm weld
Angle-to-gusset connections	3.9	2.6	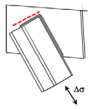	Secondary members Weld Connection					

3.4.2 Damage Assessment and Palmgren-Miner Rule

Once the structural analysis was complete for all wind speeds during the investigation, the member end forces resulting from the FE solution were collected for each structural component associated with a wind speed. The axial stress was calculated in each critical component, as shown in Table 3.5, and the resulting stress was amplified using the DAF. Then each critical member was associated with an appropriate *S-N* curve to calculate the required number of cycles to failure. Fractional damage was calculated using the Palmgren-Miner rule in Equation 3.8 to estimate the damage consumption by finding the ratio of the number of the structure's stress cycles to the number of cycles required for failure. As indicated by the *S-N* curve, only stresses greater than the threshold were assumed to contribute to the damage.

$$D_i = \frac{n_i}{N_i}$$

Equation 3.8

Where D_i is the damage in a specific member at a particular stress range, n_i is the number of cycles at *i–th* stress range (from Rainflow analysis), and N_i is the number of cycles to failure at the same stress range.

This study generated wind-time histories for 45 years of data (Al Shboul et al., 2021). These histories represented highly irregular variations of speed with time. The Rainflow counting technique (Matsuishi & Endo, 1968) was used to convert the irregular time histories to cycles, and cumulative damage was determined by adding all fractional damages associated with each wind speed using:

$$D = \sum_i D_i$$

Equation 3.9

Table 3.5: Stress Calculation in Various Structure Spots

Location	Example	Stress
Main members	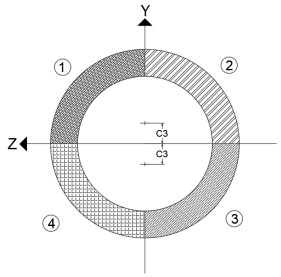	$\sigma_{x1} = \frac{My}{2C_3\frac{\pi}{2}(r_o{}^2 - r_i{}^2)} - \frac{Mz}{2C_3\frac{\pi}{2}(r_o{}^2 - r_i{}^2)}$ $\sigma_{x2} = \frac{-My}{2C_3\frac{\pi}{2}(r_o{}^2 - r_i{}^2)} - \frac{Mz}{2C_3\frac{\pi}{2}(r_o{}^2 - r_i{}^2)}$ $\sigma_{x3} = \frac{-My}{2C_3\frac{\pi}{2}(r_o{}^2 - r_i{}^2)} + \frac{Mz}{2C_3\frac{\pi}{2}(r_o{}^2 - r_i{}^2)}$ $\sigma_{x4} = \frac{My}{2C_3\frac{\pi}{2}(r_o{}^2 - r_i{}^2)} + \frac{Mz}{2C_3\frac{\pi}{2}(r_o{}^2 - r_i{}^2)}$
Post	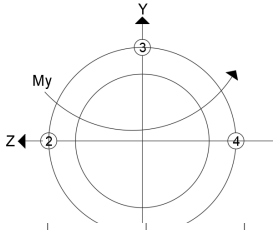	$\sigma_x = \frac{My.r}{I} + \frac{Fx}{A}$
Arm weld	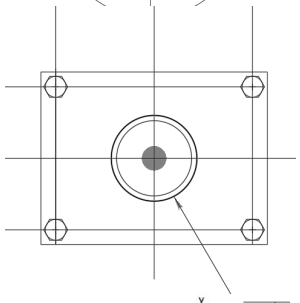	$\sigma_x = \frac{\pm My}{2C_3\frac{\pi}{2}(r_o{}^2 - r_i{}^2)} \pm \frac{Mz}{2C_3\frac{\pi}{2}(r_o{}^2 - r_i{}^2)}$ $\sigma_w = \sigma_x \frac{t_m}{t_{w3}}$
Connection bolts	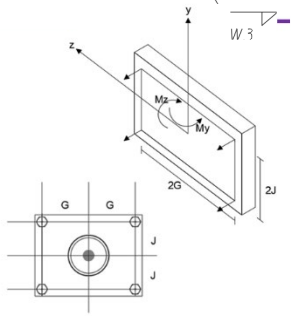	$\sigma_x = \frac{My}{4G\frac{\pi}{4}d_b{}^2} + \frac{Mz}{4J\frac{\pi}{4}d_b{}^2} + \frac{T}{4\frac{\pi}{4}d_b{}^2}$

Location	Example	Stress
Secondary members	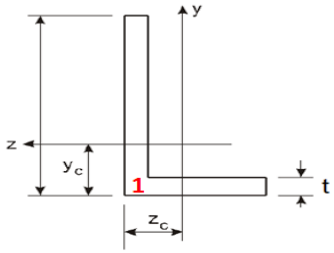	$\sigma_{x1} = -y\frac{M_z I_{yy} + M_y I_{yz}}{I_{yy}I_{zz} - I_{yz}^2} + z\frac{M_y I_{zz} + M_z I_{yz}}{I_{yy}I_{zz} - I_{yz}^2} + \frac{Fx}{A}$
Base plate weld	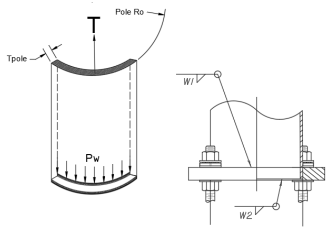	$\sigma_x = \frac{\pm My}{2C_3\frac{\pi}{2}(r_o{}^2 - r_i{}^2)} \pm \frac{Mz}{2C_3\frac{\pi}{2}(r_o{}^2 - r_i{}^2)}$ $\sigma_w = \sigma_x \frac{t_p}{t_{w1} + t_{w2}}$
Connection weld	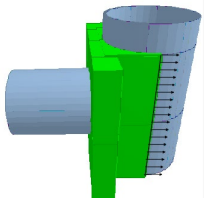	$\sigma_w = S_x \frac{t_p}{t_w}$

3.5 Analysis Automation

Figure 3.10 presents the flowchart for the developed procedures in this study. The current environment requires the user to input structure geometry, sign placement, and wind data, followed by analysis of the analytical model after exposing it to various wind speeds depending on structure location, built time, and inspection year. Automation for these steps was developed via user-friendly software written in C# to efficiently perform simulations and damage calculations. The user can specify the structure type, provide necessary geometric parameters, execute the analysis, and display the results. Figure 3.11 shows the developed software interface and the main input parameters. The user can also specify if any components experienced corrosion by selecting a thickness reduction factor to account for various levels of corrosion based on engineering judgment.

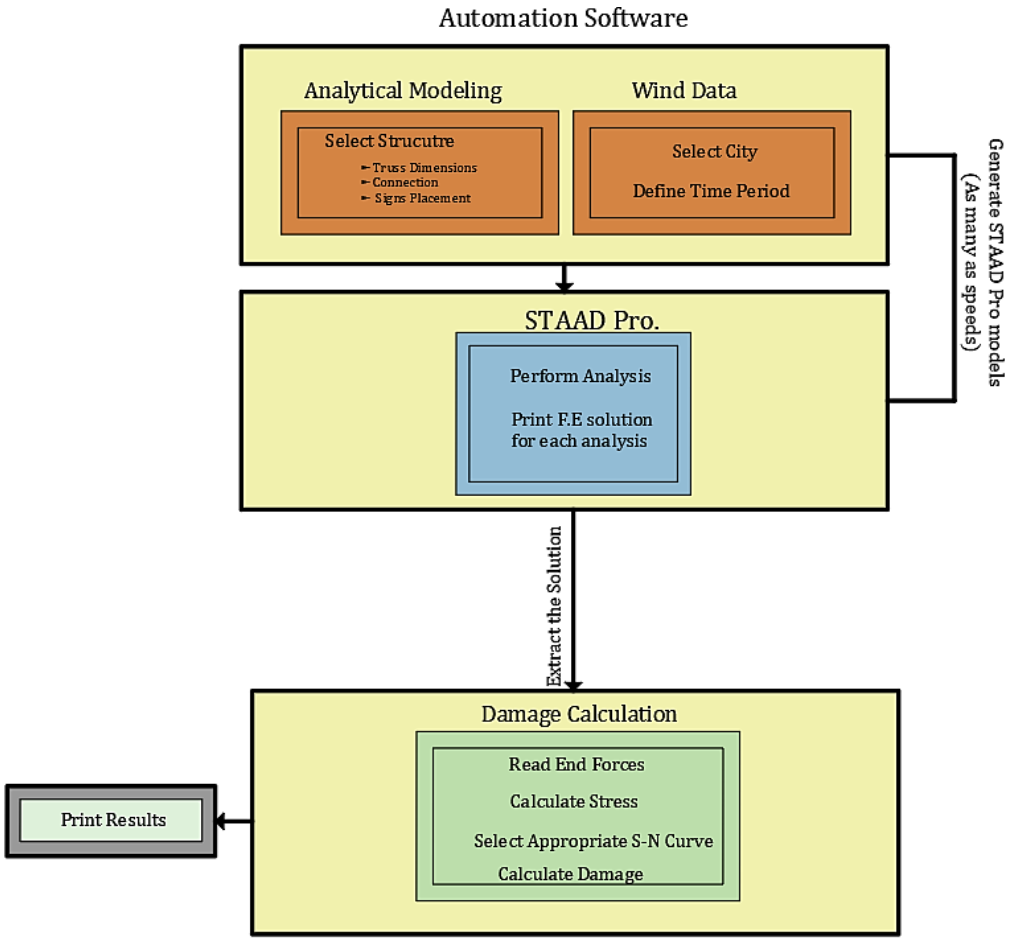

Figure 3.10: Flowchart of the Automation Algorithm

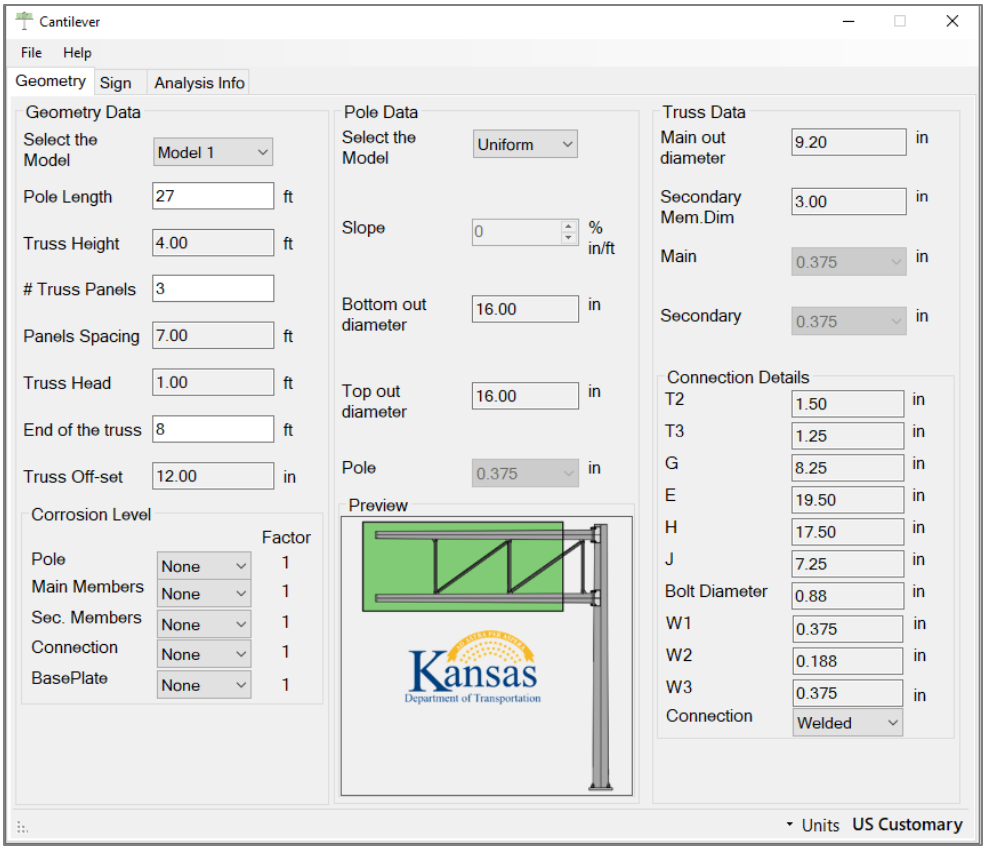

Figure 3.11: Modeling Software Interface

3.6 Evaluation of a Damaged Structure and Software Validation

3.6.1 Background

A 32-year-old cantilever highway sign structure was used to test the validity of the developed approach. This structure is in Sedgwick County, Kansas, over northbound I-235 at the ramp to West Street. The structure consists of three panels spaced at 7 ft (2133.6 mm) and supported over a single tapered post with a height of 27 ft (8229.6 mm) and base outer diameter of 16 in. (406.4 mm). The main truss has design model 1 properties and consists of multiple angle sections (3” × 3” × 3/8”) connected by welded angle-to-gusset connections. General structure properties are presented in Table 3.6, and full geometric details are shown in Figure 3.12.

Table 3.6: Sedgwick Structure Information

Structural Data		Original project data		Sign and attachment		
Structure type	Cantilever	Date let	1987	Sign ID	Sign height (ft)	Sign length (ft)
Structure material	Galvanized Steel	Inspection Date	10/30/2019	12737	6.5	12.5
Arm truss span	30 ft			12738	2.5	7.5
Vertical clearance	18 ft					

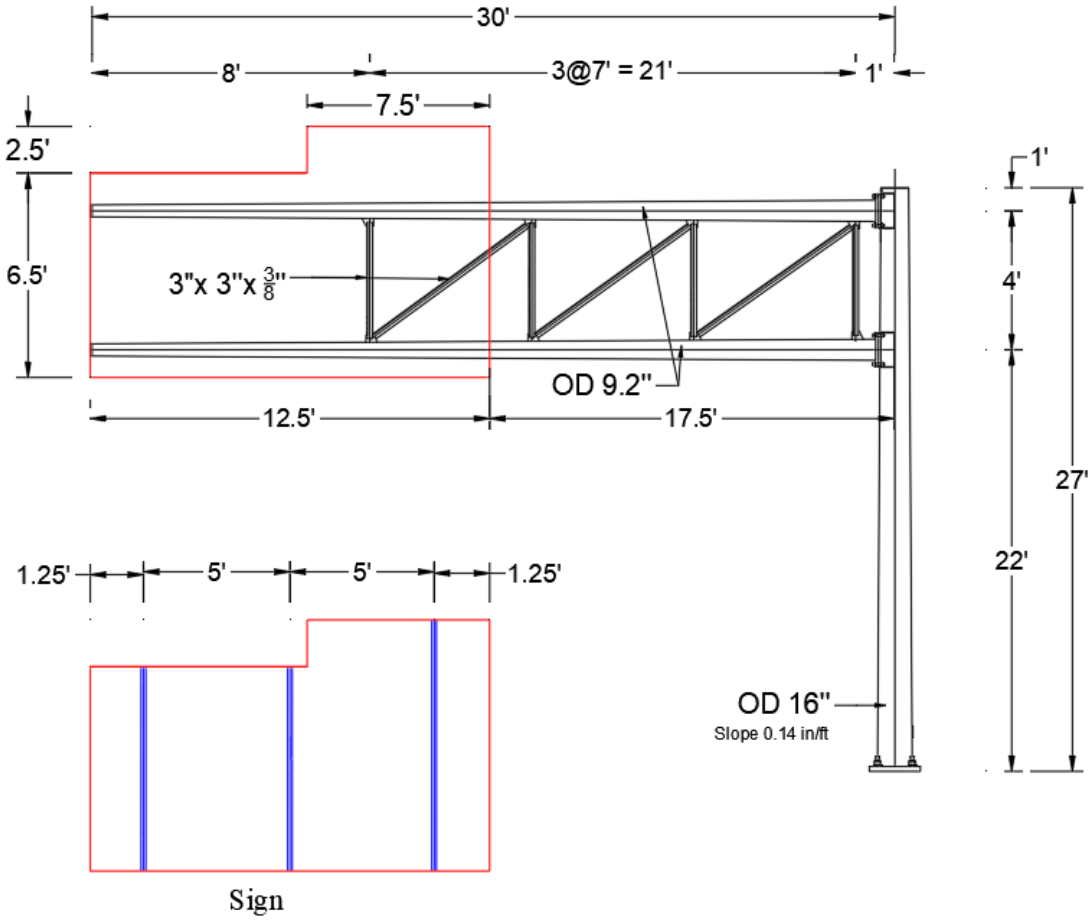

Figure 3.12: Sedgwick Structure Geometry (feet/inches)

3.6.2 Field Inspection of the Structure

On October 30, 2019, KDOT performed a comprehensive field inspection to assess the condition of all structure components as part of their regular inspection plans. The visual inspection revealed different corrosion levels for the entire structure: 50% corrosion staining was observed on anchor bolts hardware, and full corrosion staining was observed on the full height of the column. The connection plates also had corrosion staining reflected through corrosion bleed-out emanating from the weld copings. A complete fatigue crack in the vertical weld of mast-to-arm box connection at the upper chord level was also observed. A close-up view of the vertical column-to-mast arm connection is shown in Figure 3.13. The crack occurred in the entire weld toe, resulting in a complete separation of the vertical splice plate from the column.

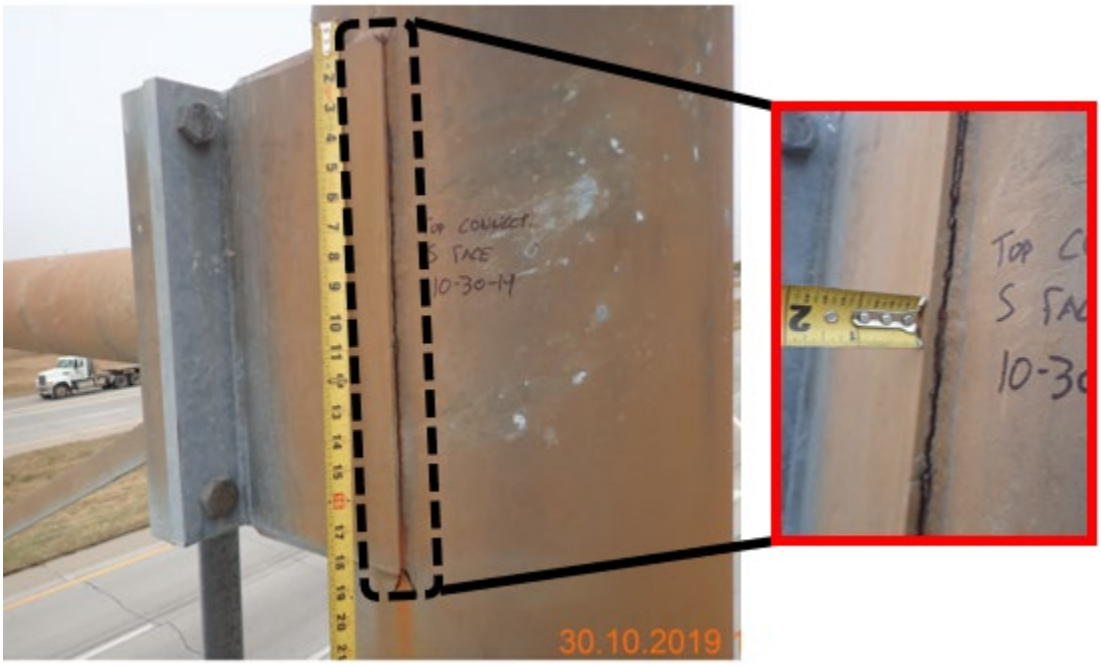

Figure 3.13: Crack in Weld Toe in Sedgwick Structure
Image courtesy of Kansas Department of Transportation (KDOT), Bureau of Structural and Geotechnical Services

3.6.3 Analytical Investigation

AASHTO (2015) has recommended infinite life specifications for mast arm-to-post connections, as well as fillet-welded and ring-stiffened boxes. This study tested these connections experimentally in full size, but they did not develop any fatigue cracking under in-plane and out-of-plane loading scenarios. However, in all the tested specimens fatigue cracking occurred in other critical locations, such as the tube-to-transverse-plate welds in the mast arm and/or the post and/or hand holes (AASHTO, 2015; Roy et al., 2011). According to AASHTO specifications, the connection between the side plate and the post was categorized as *E`* with a CAFT of 2.6 ksi (18 Mpa). The-wind loading event for the entire structure life revealed a range of wind speeds (1–33 mph), with the corresponding number of cycles the structure may experience.

After providing the software with the necessary information, including an approximated average corrosion reduction factor of approximately 17% that reflects the existing structure conditions, the software began to build and run the analysis. Following the required successive analysis by STAAD pro, the software classified the end forces for each component. The fatigue engine evaluated the fatigue life consumption for each component in the model and displayed the results in the results screen, as shown in Figure 3.14. Based on Miner's rule, the stressed component approaches the end of its life when the cumulative damage index exceeds unity. Thus, the end of fatigue life was detected only for the mast-to-arm connection (colored in red) with a damage index of 1.116.

The stress variation with wind speed for the connection and the wind-speed cycles were plotted in Figure 3.15. The stress-life method assumed that stresses greater than CAFT (2.6 ksi for this connection) contribute to fatigue damage accumulation. As shown in the figure, only stresses resulting from wind speeds of 21–33 mph will cause fatigue damage. The number of cycles to failure associated with each stress was calculated using the *S*-*N* equation with $A' = 3.29\times10^8$ ksi. Information shows the fatigue damage calculation as per Miner's rule. The possibility of a complete fatigue crack is likely due to the poor quality of the weld, meaning defects are very likely, resulting in local stress concentration and rapid fatigue damage accumulation. Moreover, the harsh corrosion environment introduced discontinuities along the weld length, leading to significantly reduced fatigue resistance.

The geographical area also significantly impacted the analysis results since the variation in fatigue life is extremely correlated to the difference in wind environment. Sedgwick County is known to have strong wind records, and many ancillary structures have shown various levels of wind-related distress as per KDOT. In addition, wind-induced fatigue damage was evaluated for all critical spots in the structure, namely, post-to-base plate weld connection, chord-to-transverse plate weld connection, anchor bolts, and all truss members. The fatigue lives of all details were found to be infinite for this particular structure, meaning that, at lower wind speeds, all stresses experienced by these details were below the threshold stress, so no fatigue damage developed. However, high wind speeds cause stresses to exceed the threshold, leading to a tendency to develop fatigue damage, but the number of cycles was low enough to prevent significant damage, resulting in infinite life.

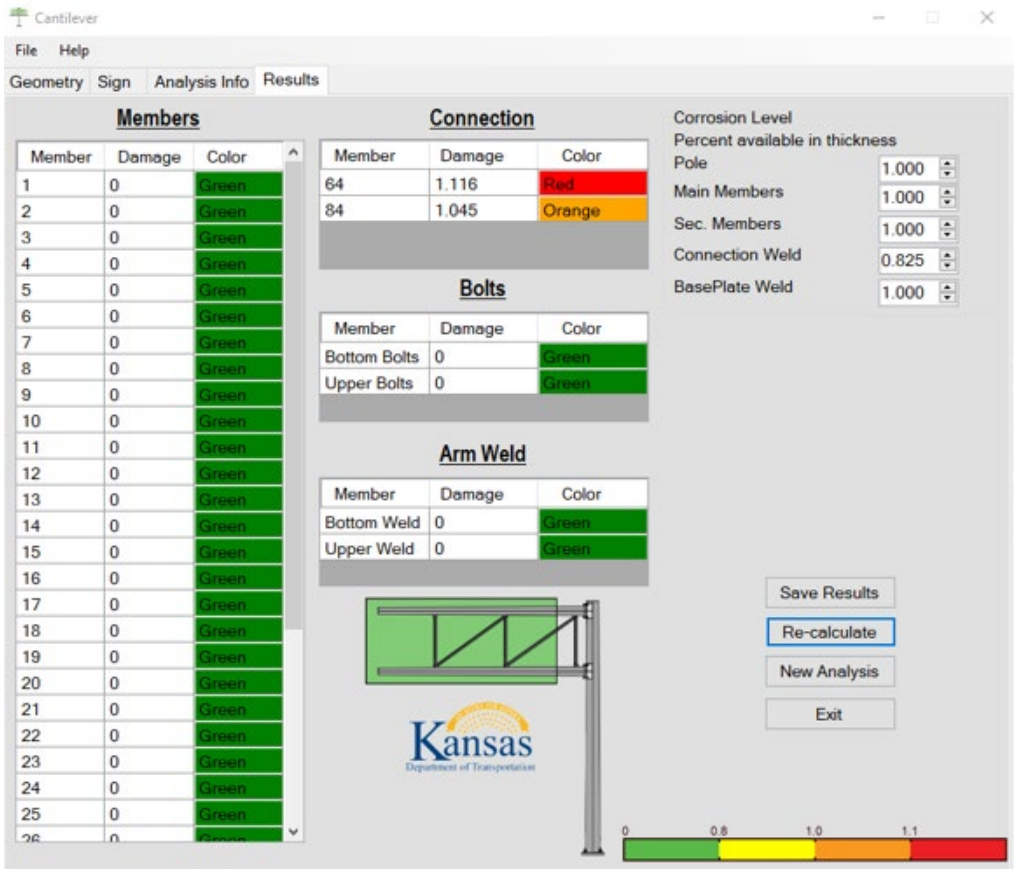

Figure 3.14: Fatigue Life Results in Sedgwick Structure

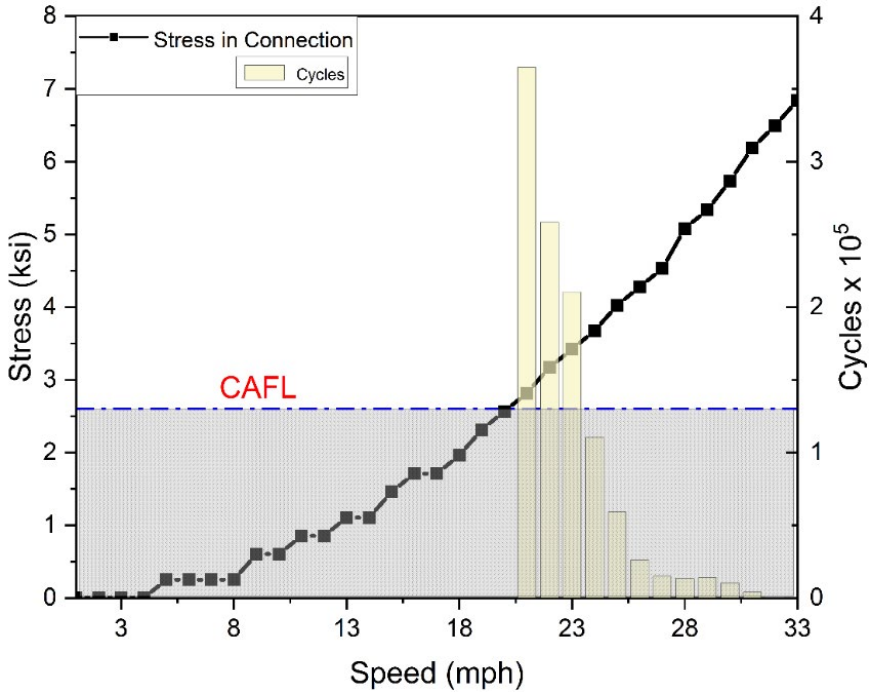

Figure 3.15: Stress Variation With Wind Speed in the Connection

Table 3.7: Stress and Damage in Connection With Wind Speed

Speed (mph)	Stress (ksi)	N_i (Cycle)	n_i (Cycle)	D_i
21	2.82	17421692.22	3647732	0.2094
22	3.17	12235811.27	2582522	0.2111
23	3.42	9730332.478	2102996	0.2161
24	3.67	7864766.583	1105565	0.1406
25	4.03	5975640.433	590647.5	0.0988
26	4.28	4981930.229	260106	0.0522
27	4.53	4196883.267	149004	0.0355
28	5.08	2969547.639	133981.5	0.0451
29	5.33	2568838.623	138694.5	0.0540
30	5.74	2065094.187	102642	0.0497
31	6.19	1644141.092	40464	0.0246
32	6.49	1425231.089	4365	0.0031
33	6.84	1216291.56	405	0.0003
				Sum = 1.1

This study developed identical software for butterfly sign structures. The fatigue life for butterfly truss members was recalculated using the software to compare the analytical results with the actual condition of a structure in Wyandotte County, Kansas. Truss details and the structure model are shown in Table 3.8 and Figure 3.16, respectively. After completing the required analysis, the results screen indicated no component experienced fatigue damage (Figure 3.17).

Table 3.8: Wyandotte Structure Information

Structural Data		Original project data		Sign and attachment		
Structure type	Butterfly	Date let	1985	Sign ID	Sign height (ft)	Sign length (ft)
Structure material	Galvanized Steel	Inspection Date	8/6/2019	---	8.5	18
Arm truss span	10 ft					
Vertical clearance	0 ft					

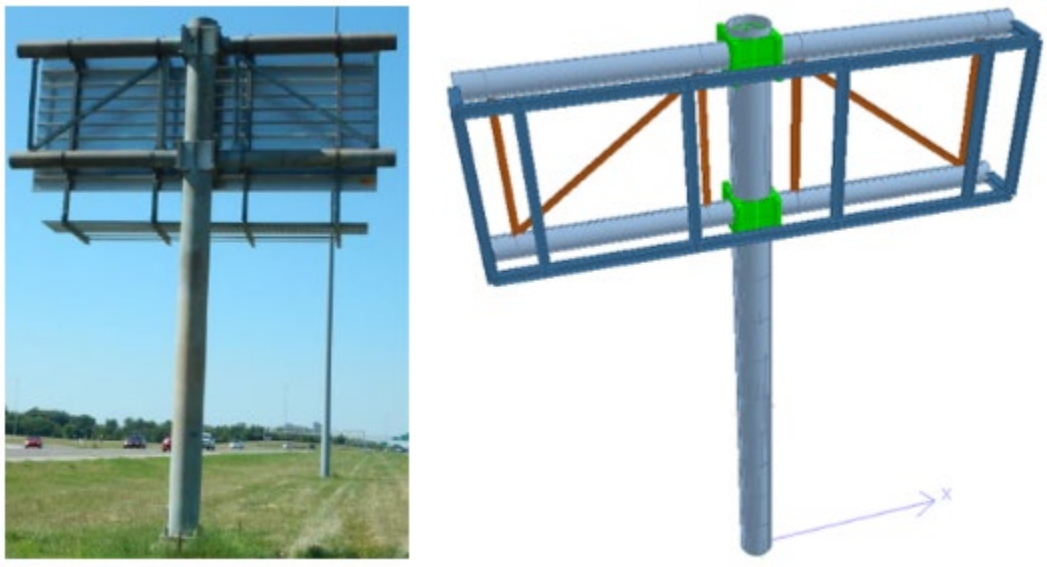

(a) (b)

Figure 3.16: (a) Actual Structure, (b) Model

Figure 3.17: Damage in the Butterfly Member's Model

Chapter 4: Conclusions and Recommendations

This study developed and implemented a framework for analytical fatigue damage evaluation in computer software to provide a cost-effective inspection tool to assess highway sign structures. Analytical models were created for a cantilever structure based on wind-event history to simulate damage in various critical truss components. The software showed its superior capability in calculating fatigue damage by capturing a crack in the mast connection. The main conclusion is that the most critical fatigue detail is the connection because it has lower CAFT and is susceptible to high stress.

KDOT standards recommend replacing the gusseted box connection with the ring-stiffened connection due to the superior resistance of the latter to fatigue damage. Accurate fatigue damage characterization is highly dependent on actual past wind events during the service life of the structure. Fatigue failure has been widely noticed in flexible highway sign structures, and it is essential to alert highway agencies to faulty connections in an efficient and timely manner. Therefore, this developed software should beneficially impact state highway decision-making and the development of inspection inventories.

References

Al Shboul, K. W., Rasheed, H. A., & AlKhiary, A. (2023). Spatial wind speed interpolation using isoparametric shape functions for structural loading. *Structures*, *50*, 444–463. https://doi.org/10.1016/j.struc.2023.02.037

Al Shboul, K. W., Rasheed, H. A., & Alshareef, H. A. (2021). Intelligent approach for accurately predicting fatigue damage in overhead highway sign structures. *Structures*, *34*, 3453–3463. https://doi.org/10.1016/j.struc.2021.09.090

Alshareef, H. A., Al Shboul, K. W., Rasheed, H. A., & Abouelleil, A. (2022). Analytical-based application software for estimating remaining fatigue life of non-cantilevered sign structures. *Engineering Structures*, *262*, Article 114315. https://doi.org/10.1016/j.engstruct.2022.114315

American Association of State Highway and Transportation Officials (AASHTO). (1994). *Standard specifications for structural supports for highway signs, luminaires and traffic signals*.

American Association of State Highway and Transportation Officials (AASHTO). (2015). *2015 interim revisions to standard specifications for structural supports for highway signs, luminaires and traffic signals* (6th ed.).

American Welding Society (AWS). (2000). *Structural welding code – steel* (AWS D1.1:2000) (17th ed.).

Barle, J., Grubisic, V., & Vlak, F. (2011). Failure analysis of the highway sign structure and the design improvement. *Engineering Failure Analysis*, *18*(3), 1076–1084. https://doi.org/10.1016/j.engfailanal.2011.02.006

Ben-Israel, A., & Greville, T. N. E. (2003). *Generalized inverses: Theory and applications* (2nd ed.). Springer.

Beneberu, E., Goode, J., & Yazdani, N. (2014). Computational fluid dynamics application for design of highway sign support structures. *International Journal of Civil and Structural Engineering*, *5*(2), 101–111. https://www.researchgate.net/publication/275893563

Bentley Systems. (2016). Staad Pro V8i SS6 [Computer software]. https://www.bentley.com/software/staad

Bobillier, B., Chakrabarti, S., & Christiansen, P. (2001). Physical modeling of wind load on a floating offshore structure. *Journal of Offshore Mechanics and Arctic Engineering*, *123*(4), 170–176. https://doi.org/10.1115/1.141/1770-24

Chen, G., Wu, J., Yu, J., Dharani, L. R., & Barker, M. (2001). Fatigue assessment of traffic signal mast arms based on field test data under natural wind gusts. *Transportation Research Record*, *1770*, 188–194. https://doi.org/10.3141/1770-24

Choi, H., & Najm, H. (2018). Fatigue reliability assessment of potential crack initiation of tube-to-transverse plate connections for cantilever sign support structures. *Journal of Performance of Constructed Facilities*, *32*(2), Article 04018002. https://doi.org/10.1061/(ASCE)CF.1943-5509.0001139

Creamer, B. M., Frank, K. H., & Klingner, R. E. (1979). *Fatigue loading of cantilever sign structures from truck wind gusts* (Report No. FHWA/TX-79/10+209-1F). University of Texas at Austin, Center for Highway Research. https://library.ctr.utexas.edu/digitized/texasarchive/phase2/209-1F-CHR.pdf

Davenport, A. G. (1961). The spectrum of horizontal gustiness near the ground in high winds. *Quarterly Journal of the Royal Meteorological Society*, *87*(372), 194–211. https://doi.org/10.1002/qj.49708737208

DeSantis, P. V., & Haig, P. E. (1996). Unanticipated loading causes highway sign failure. In A. Ali et al. (Eds.), *1996 ANSYS Conference proceedings*. ANSYS, Inc.

Dexter, R. J., & Ricker, M. J. (2002). *Fatigue-resistant design of cantilevered signal sign, and light supports* (NCHRP Report 469). Transportation Research Board. https://onlinepubs.trb.org/onlinepubs/nchrp/nchrp_rpt_469-a.pdf

Florea, M. J., Manuel, L., Frank, K. H., & Wood, S. L. (2007). *Field tests and analytical studies of the dynamic behavior and the onset of galloping in traffic signal structures* (Report No. FHWA/TX-08/0-4586-1). University of Texas at Austin, Center for Highway Research. https://library.ctr.utexas.edu/ctr-publications/0-4586-1.pdf

Fouad, F. H., & Hosch, I. E. (2011). *Design of overhead VMS structures for fatigue loads* (Report No. 09203). University of Alabama, University Transportation Center for Alabama. https://rosap.ntl.bts.gov/views/dot/25439

Ginal, S. (2003). *Fatigue performance of full-span sign support structures considering truck-induced gust and natural wind pressures* (Master's thesis). Marquette University.

Hamilton III, H. R., Puckett, J. A., Gray, B., Wang, P., Deschamp, B., & McManus, P. (2004). *Traffic signal pole research* (Report No. FHWA-WY-04/03F). Wyoming Department of Transportation. https://ntrl.ntis.gov/NTRL/dashboard/searchResults/titleDetail/PB2005100661.xhtml

Hong, H. P., Zu, G. G., & King, J. P. C. (2016). Estimating fatigue design load for overhead steel sign support structures under truck-induced wind pressure. *Canadian Journal of Civil Engineering*, *43*(3), 279–286. https://doi.org/10.1139/cjce-2015-0158

Hosseini, M. S. (2013). *Parametric study of fatigue in light pole structures* (Master's thesis). University of Akron. http://rave.ohiolink.edu/etdc/view?acc_num=akron1374530021

Iannuzzi, A., & Spinelli, P. (1987). "Artificial wind generation and structural response." *Journal of Structural Engineering*, *113*(12), 2382–2398. https://doi.org/10.1061/(ASCE)07339445(1987)113:12(2382)

Kacin, J., Rizzo, P., & Tajari, M. (2010). "Fatigue analysis of overhead sign support structures." *Engineering Structures*, *32*(6), 1659–1670. https://doi.org/10.1016/j.engstruct.2010.02.014

Kaczinski, M. R., Dexter, R. J., & Van Dien, J. P. (1998). *Fatigue-resistant design of cantilevered signal, sign and light supports* (NCHRP Report 412). Transportation Research Board. https://onlinepubs.trb.org/onlinepubs/nchrp/nchrp_rpt_412.pdf

Kaimal, J. C., Wyngaard, J. C., Izumi, Y., & Coté, O. R. (1972). Spectral characteristics of surface-layer turbulence. *Quarterly Journal of the Royal Meteorological Society*, *98*(417), 563–589. https://doi.org/10.1002/qj.49709841707

Kumar, K. S., & Stathopoulos, T. (1997). Computer simulation of fluctuating wind pressures on low building roofs. *Journal of Wind Engineering and Industrial Aerodynamics*, *69*, 485–495. https://doi.org/10.1016/S0167-6105(97)00179-7

Letchford, C. J., & Cruzado, H. (2008). *Risk assessment model for wind-induced fatigue failure of cantilever traffic signal structures* (Report No. FHWA/TX-07-4586-4). Texas Tech University, Center for Multidisciplinary Research in Transportation. https://rosap.ntl.bts.gov/view/dot/66522

Li, X. (2005). *Fatigue strength and evaluation of highway sign structures* (Doctoral dissertation). Purdue University.

Li, X., Whalen, T. M., & Bowman, M. D. (2005). Fatigue strength and evaluation of double-mast arm cantilevered sign structures. *Transportation Research Record*, *1928*, 64–72. https://doi.org/10.1177/0361198105192800107

Luo, W., Taylor, M. C., & Parker, S. R. (2008). A comparison of spatial interpolation methods to estimate continuous wind speed surfaces using irregularly distributed data from England and Wales. *International Journal of Climatology*, *28*(7), 947–959. https://doi.org/10.1002/joc.1583

Matsuishi, M., & Endo, T. (1968). Fatigue of metals subjected to varying stress. *Preliminary proceedings of the Kyushu District Meeting, Fukuoka, March 1968* (Vol. 2, pp. 37–40). Japan Society of Mechanical Engineers.

Puckett, J. A., Erikson, R. G., & Peiffer, J. P. (2010). Fatigue testing of stiffened traffic signal structures. *Journal of Structural Engineering*, *136*(10), 1205–1214. https://doi.org/10.1061/(ASCE)ST.1943-541X.0000229

Repetto, M. P., & Solari, G. (2001). Dynamic alongwind fatigue of slender vertical structures. *Engineering Structures*, *23*(12), 1622–1633. https://doi.org/10.1016/S0141-0296(01)00021-9

Rice, J. A., Foutch, D. A., LaFave, J. M., & Valdovinos, S. (2012). Field testing and analysis of aluminum highway sign trusses. *Engineering Structures*, *34*, 173–186. https://doi.org/10.1016/j.engstruct.2011.09.021

Roda, A. M., Najm, H., & Choi, H. (2015). *Fatigue study on structural supports for luminaries* [sic]*, traffic signals, highway signs (LRFD LTS)*. New Jersey Department of Transportation. https://dx.doi.org/10.13140/RG.2.2.23638.24648

Roy, S., Park, Y. C., Sause, R., Fisher, J. W., & Kaufmann, E. J. (2011). *Cost-effective connection details for highway sign, luminaire, and traffic signal structures* (NCHRP Web-Only Document 176). Transportation Research Board. https://doi.org/10.17226/22879

Simiu, E., & Scanlan, R. H. (1996). *Wind effects on structures: Fundamentals and applications to design* (3rd ed.). John Wiley.

Tsai, L.-W., & Alipour, A. (2021). Studying the wind-induced vibrations of a traffic signal structure through long term health monitoring. *Engineering Structures*, *247*, Article 112837. https://doi.org/10.1016/j.engstruct.2021.112837

Webster, R., & Oliver, M. A. (2007). *Geostatistics for environmental scientists* (2nd ed.). Wiley.

Ye, W. (2013). *Spatial variation and interpolation of wind speed statistics and its implication in design wind load* (Post-graduate thesis). University of Western Ontario. https://hdl.handle.net/20.500.14721/37810

Zheng, R., & Ellingwood, B. R. (1998). Stochastic fatigue crack growth in steel structures subject to random loading. *Structural Safety*, *20*(4), 303–323. https://doi.org/10.1016/S0167-4730(98)00020-4

K-TRAN

KANSAS TRANSPORTATION RESEARCH AND NEW-DEVELOPMENT PROGRAM

AD ASTRA PER ASPERA

Kansas

Department of Transportation